J. Physiol. (1979), **288**, *pp.* 589–611
With 1 *plate and* 13 *text-figures*
Printed in Great Britain

THE MEMBRANE CURRENT OF SINGLE ROD OUTER SEGMENTS

BY D. A. BAYLOR, T. D. LAMB* AND K.-W. YAU*

From the Department of Neurobiology, Stanford University School of Medicine, Stanford, California 94305, U.S.A.

(*Received 29 March 1978*)

SUMMARY

1. Outer segments of individual rods in the retina of the toad, *Bufo marinus*, were drawn into a glass pipette to record the membrane current.

2. Light flashes evoked transient outward currents. The peak response amplitude was related to flash intensity by a Michaelis equation with half-saturating intensity about 1 photon μm^{-2}.

3. The saturating response amplitude ranged up to 27 pA and corresponded closely to complete suppression of the steady inward current present in darkness.

4. For a given cell the saturating response amplitude varied linearly with the length of outer segment within the pipette. This is consistent with a uniform density of light-sensitive channels and negligible gradient of membrane potential along the outer segment.

5. Responses to bright flashes never showed the relaxation from an initial peak seen previously in intracellular voltage recordings, suggesting that the conductance change responsible for the relaxation does not occur in the outer segment.

6. Responses to local illumination of only the recorded outer segment were very similar to those obtained with diffuse light at the same intensity, indicating that peripheral rods made little contribution to the responses.

7. The spectral sensitivity of 'red' rods was consistent with a retinal$_1$-based pigment with $\lambda_{max} = 498 \pm 2$ nm.

8. The kinetics of the response were consistent with four stages of delay affecting action of the internal transmitter. Responses were faster at the basal end of the outer segment than at the distal tip.

9. Background light reduced the sensitivity to a superposed dim test flash and shortened the time course of the response, indicating that adapting light modifies the kinetics and gain of the transduction mechanism within the outer segment.

10. Responses to dim lights exhibited pronounced fluctuations which are attributed in the succeeding paper (Baylor, Lamb & Yau, 1979) to the quantal nature of light.

INTRODUCTION

It is generally accepted that the hyperpolarizing light response of vertebrate photoreceptors results from reduction in a steady inward current of sodium ions which in darkness flows across the outer segment membrane. The electrical responses

* Present address: Physiological Laboratory, University of Cambridge, Cambridge CB2 3EG.

of receptors have been studied by measurement of extracellular voltage gradients (Hagins, Penn & Yoshikami, 1970) and by intracellular voltage recording (Tomita, 1970). Such measurements provide information averaged over a number of cells because of the high extracellular conductivity and the existence of electrical coupling between photoreceptors (Baylor, Fuortes & O'Bryan, 1971; Baylor & Hodgkin, 1973; Copenhagen & Owen, 1976; Fain, Gold & Dowling, 1976; Schwartz, 1976; Lamb & Simon, 1976).

There are two incentives to recording the membrane current of a single photoreceptor's outer segment. Firstly, the technique should help to determine which regions of the cell membrane are responsible for generating the dark noise (Simon, Lamb & Hodgkin, 1975; Lamb & Simon, 1976, 1977; Schwartz, 1977) and for causing the spike-like transient in intracellular voltage responses to bright flashes (Baylor *et al.* 1971; Kleinschmidt, 1973; Schwartz, 1973; Brown & Pinto, 1974; Baylor, Hodgkin & Lamb, 1974; Fain, 1975). Secondly, the technique permits observation of responses to single photons, a level of resolution not attainable with intracellular recording because electrical coupling averages the responses of many cells and severely reduces the amplitude of individual events.

In the present study, the membrane current of a single outer segment has been recorded; 'red' rods in the retina of the toad, *Bufo marinus*, have been studied because of their large size. This paper describes general properties of the membrane current, while the following paper (Baylor *et al.* 1979) deals with responses to single photons.

A preliminary description of some of this work has been reported previously (Yau, Lamb & Baylor, 1977). A similar recording technique has been used by Jagger (1976) and McBurney and Normann (1977).

METHODS

Optical system. Text-fig. 1*A* is a schematic diagram of the apparatus for electrical recording and optical stimulation of single outer segments. A glass chamber, C, containing the pieces of retina was mounted on the stage of an inverted compound microscope (Zeiss Invertoscope D). The prism above, P_1, directed light from a dual-beam optical stimulator (similar to that of Baylor & Hodgkin, 1973) downwards, through the polarizer, Pol, condensing lens, CL (Zeiss Phako IV Z7 'J'), and onto the preparation. In most of the experiments described in this paper the light was plane-polarized with the plane of polarization normal to the long axis of the outer segment (i.e. in the 'preferred' direction); in other experiments the light was not polarized. Light collected by the objective, O (Zeiss planachromat, 6·3, 16 or 40 ×) was directed by prism P_3, either to the viewing eye-pieces, EP (Zeiss, 25 × KPL), or to a side tube. An infra-red image converter, IR (Metascope, Varo Inc.), was mounted behind one eye-piece, and an infra-red filter (Schott, RG850) was placed in one or both beams of the optical stimulator. It was possible to connect to the side tube of the microscope either a camera or a quantum photometer (Princeton Applied Research 1140A/B). Unless otherwise stated the stimulus was 500 nm 'monochromatic' light. Light calibration was performed at the end of each experiment by placing the sensor of a photometer (United Detector Technology, 111A) at the position normally occupied by the preparation. Neutral density filters were calibrated *in situ* using both photometers.

Knowledge of the stop-band properties of the 700 nm interference filter was important in spectral sensitivity measurements (see p. 600). We were unable to measure directly the high attenuation in the skirt of the interference filter (i.e. of the order of 5 or more log units) and resorted to the following procedure. The threshold of detection for a dark-adapted human observer was determined with light from the optical bench transmitted through a broadband green interference filter (λ_{max} = 542 nm, half width = 85 nm). A second determination was

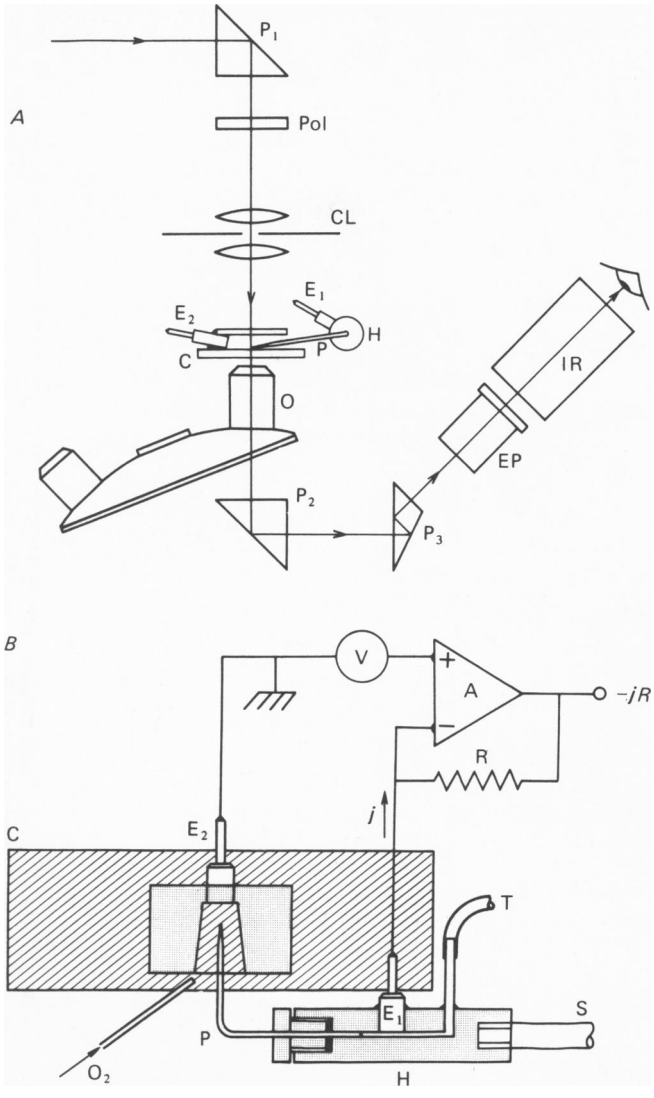

Text-fig. 1. Diagram of the stimulating and recording arrangement. *A*, optical path through the inverted compound microscope. P_1, P_2, P_3, prisms; Pol, polarizer; CL, condensing lens; C, chamber for holding retinal pieces (see 1*B*); P, pipette; H, pipette holder; E_1, E_2, Ag/AgCl electrodes; O, objective; EP, eye-piece; IR, infra-red image converter. *B*, top view of pipette holder and glass chamber for holding retinal pieces. The chamber, C, consisted of a 25 × 76 mm glass slide with a smaller piece of glass spaced about 4 mm above (see also *A*). This formed a cavity sealed on three sides (stipple), but open at the front, and the Ringer solution containing retinal pieces was held in by surface tension. P, pipette, H, pipette holder; E_1, E_2, Ag/AgCl electrodes; S, shaft for connexion to micromanipulator; T, tubing for connexion to pressure system. O_2, tube for blowing moist oxygen against surface of Ringer solution. The current, j, was monitored by amplifier A with feed-back resistance, R = 100 MΩ; V, voltage source, variable continuously and stepwise.

made with the 700 nm interference filter in series with the broadband filter and required the removal of 6·6 log units of attenuation in order to reach threshold; at slightly higher intensities the beam appeared red. Allowing for the fact that the 700 nm filter attenuated by approximately 0·3 log units at 700 nm, we interpret this result to indicate that in the band 500–580 nm the 700 nm filter attenuated by more than a factor of 10^6.

Recording chamber and pipette holder. The glass chamber, C (see Text-fig. 1*B*), was open-fronted, and the Ringer solution containing the preparation remained within by surface tension. The chamber was placed in the microscope's slide holder and could be finely positioned in the horizontal plane. The pipette, P, was gripped by the holder, H, on which was mounted a Ag/AgCl electrode, E_1, suction being applied via the tubing, T. The holder was mounted on a Leitz micromanipulator by shaft, S.

Electrical recording. The recording arrangement, based on that of Neher & Sakmann (1976), is shown diagrammatically in Text-fig. 1*B*. The current, j, flowing between the Ag/AgCl electrodes, E_1 and E_2, was monitored by amplifier A (Function Modules, 380K), which produced an output voltage, $-jR$, with the feed-back resistance $R = 100$ MΩ. The variable voltage source, V, allowed compensation for differences in electrode potentials and provided voltage steps (usually 100 μV) for measuring electrode resistance. Recording resolution was limited by thermal noise in the leakage resistance between the inner surface of the electrode tip and the membrane of the outer segment. The output signal was amplified, stored on an FM tape recorder (Ampex, PR-2200) with band width 0–312 Hz, and displayed on a chart recorder. On replay the signal was filtered by a 6-pole low-pass filter with cut-off frequency set at 15, 20, or 30 Hz. Responses were averaged with a digital computer (DEC, PDP 11/34).

Suction. Small pressure changes were made using an oil-filled system with gas-chromatography syringes (100 μl. and 1 ml.) driven by micrometers. An air bubble was left between the oil and Ringer solution in the pipette holder to prevent oil getting into the recording system; the bubble also provided a degree of compressibility, permitting finer control of the sucking action.

Pipette electrode. Pipettes with rapidly tapering shanks were pulled from 1·2 mm outer diameter Pyrex capillary glass (Corning, medium wall). They were scored with a diamond knife and broken off squarely at a position where the outer diameter was about 50 μm. While viewing the tip under a compound microscope, a platinum heating wire was brought near until the tip had collapsed to give a constricted entrance about 6 μm in inner diameter and about 10–15 μm in length (see Plate 1*A*). To prevent direct contact between glass and outer segment membrane, a thin coating of vinyl resin (Stoner-Mudge, Mobil) was applied to the pipette tip by briefly immersing it in a drop of thinned resin and then manually applying strong suction using an air-filled syringe. The resistance of a good pipette was typically 1·5–2 MΩ when filled with Ringer solution.

Ringer solution. Toad Ringer solution was that used by Brown & Pinto (1974). It contained (in mM): NaCl, 111; $MgCl_2$, 1·6; KCl, 2·5; $CaCl_2$, 1·0; D-glucose, 10; HEPES, 3, buffered to pH 7·8 with NaOH.

Temperature. All experiments were done at room temperature (18–25 °C).

Retina. Toads, *Bufo marinus*, were maintained at 25 °C on a diurnal light–dark cycle and fed new-born rats. In dim red light a toad, which had been dark-adapted overnight, was pithed and one eye was removed, the other being used several hours later. With the aid of a dissecting microscope and infra-red image converter, the posterior pole of the globe was cut off with a razor blade and cut into two or three segments, avoiding the optic disk. These segments were placed in a small dish of Ringer solution and the retina was gently isolated from each segment. The retinal segments were transferred with a broad-tipped pipette to another dish and cut with a section of razor blade into pieces about 0·1–0·2 mm in size. Each piece probably contained several hundred photoreceptors, but in many cases a substantial number of outer segments were broken off. The chopped pieces were then transferred by pipette to the glass chamber and mounted on the stage of the inverted microscope. Except for initial pithing and enucleation, the procedure was carried out without visible light. After the preparation was in place on the microscope, inside a light-tight enclosure, dim red light was used in the room.

Recording procedure. Under infra-red illumination, the chamber was scanned by moving it horizontally with the mechanical stage of the microscope. When a piece of retina with intact and suitably oriented outer segments was found, the microscope was focused on an outer segment and the pipette was adjusted to the same vertical position. While advancing the retinal

piece towards the electrode using the mechanical stage adjustment, gentle suction was applied so that the tip of the cell entered the lumen of the pipette. The stage position and the suction were then adjusted together so that the cell slipped in smoothly without buckling or stretching. Plate 1 shows a sequence of photographs taken in visible light with a cell approaching the electrode (*A*), drawn in (*B*), and illuminated with a slit applied longitudinally (*C*) and transversely (*D*). With a cell properly in place the electrode resistance was typically three to five times higher than initially, permitting 80 % or more of the membrane current to be recorded.

An electrical artifact was almost invariably encountered while sucking a cell in. It appeared as a current induced by a voltage change of up to about 100 μV, in a positive direction (i.e. current entering the pipette tip) during sucking, and in a negative direction during blowing. The sign and magnitude of the artifact were consistent with a differential pressure effect on the Ag/AgCl electrodes, but it may alternatively have arisen from a streaming potential resulting from fluid motion through the pipette tip. This artifact made it difficult to determine the steady current flowing across the cell membrane in darkness; a way around the problem is described in the Results.

Stimulation. Light was applied over the entire preparation, or locally to the recorded outer segment by imaging on it a rectangular slit of adjustable size. The image of the slit was positioned using screw carriages on the optical bench and focused by adjusting the height of the condensing lens. Although the lens was not perfectly achromatic in the range 420–850 nm, it was found that almost identical focusing was obtained with infra-red light and with the 500 nm blue-green light which was used in most experiments. The slight degree of image blurring at other wavelengths probably had little effect on the spectral sensitivity curves, which were determined with wide slits.

RESULTS

Relation of photocurrent to dark current

Text-fig. 2*A* shows the response of a red rod to a bright flash of blue-green light at time zero. The photocurrent was an outward change approximately 20 pA in amplitude which remained at the saturating level for several seconds. As discussed in the Methods, an electrical artifact which accompanied pressure changes made it impossible to determine the standing dark current from the change in current resulting when the outer segment was drawn in. To circumvent this problem the outer segment was broken from the inner segment at the cilium by delivering sharp taps to the base-plate (arrows in Text-fig. 2*A*) after the cell had recovered from the previous flash. Breakage resulted in a rapid outward change in current of about 22 pA and failure of the outer segment to respond to a second identical flash. Visual observation confirmed that the outer segment had separated from the inner segment and had not moved within the pipette.

The abrupt change in current produced by breakage of the cilium and the absence of a light response thereafter is consistent with the notion that net membrane current was abolished by breakage, as would have occurred if the membrane resealed. Assuming that the level after breakage indeed represented zero membrane current, the similar level reached in the preceding bright flash response suggests that the flash almost completely blocked a steady inward current present in darkness.

In this experiment it was necessary to ensure, before breaking the cilium, that there was no net pressure across the cell. In some attempts the detached outer segment moved in one direction or the other, and these were discounted. Text-fig. 2*B* plots collected results from eighteen stable cells. In all cases the saturating response (ordinate) was within 2 pA of the change resulting from breakage (abscissa). The line of least squares fit restricted to pass through the origin (0, 0) passes through

the mean $(\bar{x}, \bar{y})$, and for these points had a slope of 0·99; however, the line in Text-fig. 2*B* is drawn with unit slope. The conclusion from these results is that virtually the entire dark current is abolished in bright light.

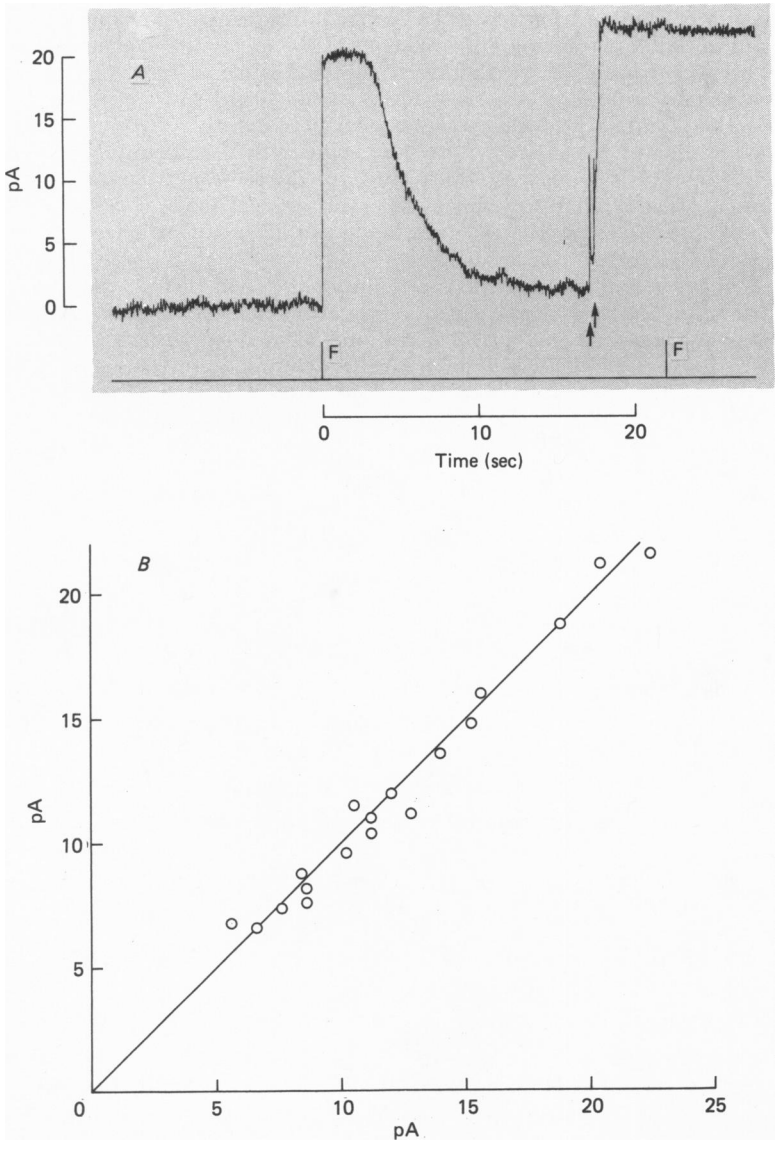

Text-fig. 2. Response to bright flash followed by severing ciliary neck of outer segment. *A*, at time zero a bright diffuse flash (F) elicited a saturating response of about 20 pA which remained at the plateau level for several seconds. After recovery two sharp taps were given to the micromanipulator base-plate (arrows), causing breakage of the cilium and a step change in current of about 22 pA. A second flash (F) then gave no response. Electrode resistance changed by less than 10 % when cell was broken. Outward membrane current plotted upwards in this and subsequent Figures. *B*, saturating light response (ordinate) against change in current on breakage (abscissa) for eighteen cells. Straight line through origin has unity slope.

Response as a function of intensity

A family of responses to a series of brief flashes of increasing intensity is shown in Text-fig. 3*A*. The lower three traces are averages of eight to twenty-two responses, while the remainder are single sweeps or averages of only a few responses. The

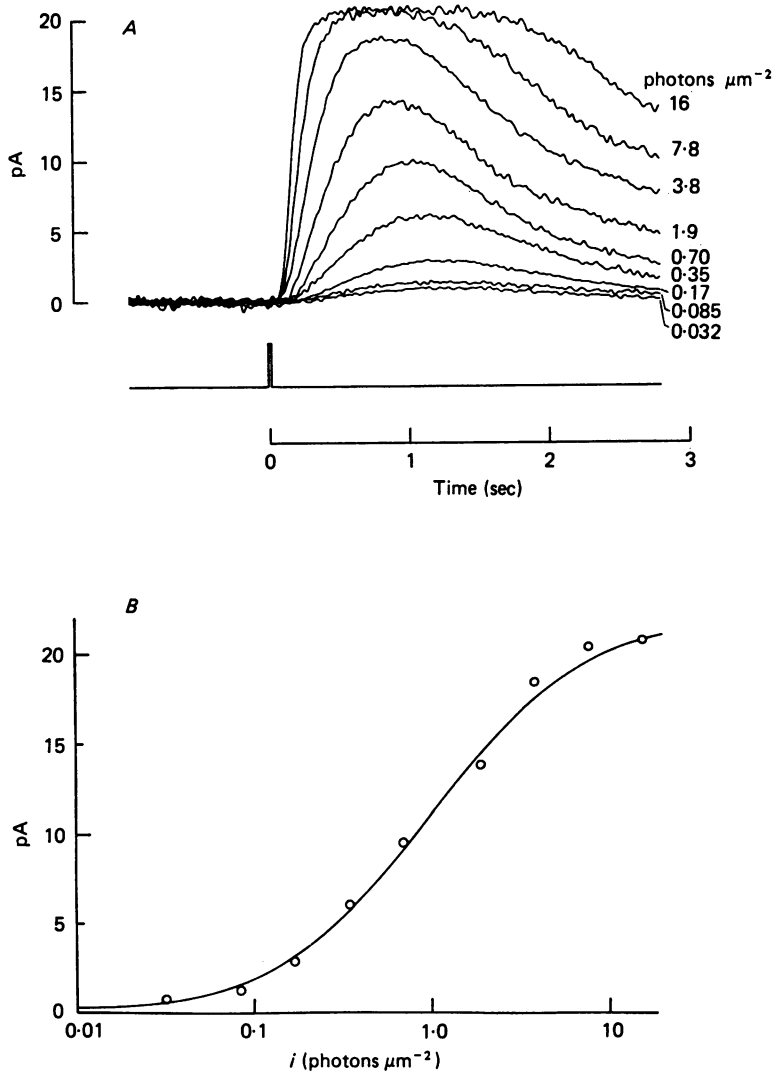

Text-fig. 3. Responses to flashes of increasing intensity. *A*, response in pA relative to the level in darkness is plotted against time from the middle of a 20 msec flash of light. Illumination applied only to the outer segment in the pipette; 500 nm monochromatic polarized light; numbers at right represent intensity in photons μm^{-2} per flash. The lowest three traces are averages of ten, eight and twenty-two responses respectively; other traces based on one to four responses. The signal was filtered by a 6-pole low-pass filter with cut-off frequency 20 Hz. Cell 9 of Table 1. *B*, peak responses from *A* plotted against flash intensity (log scale). Curve is eqn. (1) with r_{max} = 22 pA, i_0 = 1·0 photons μm^{-2}.

variation of peak amplitude with flash intensity for this cell has been plotted in Text-fig. 3*B* and is fitted by the rectangular hyperbola or Michaelis equation

$$\frac{r}{r_{max}} = \frac{i}{i+i_0}. \tag{1}$$

Here r represents response amplitude (pA), with maximum r_{max}, and i represents flash intensity (incident photons μm^{-2}) with half-saturating intensity i_0. The flash intensity i is related to the steady intensity I (photons μm^{-2} sec^{-1}) by $i = I\Delta t$, where Δt is the flash duration.

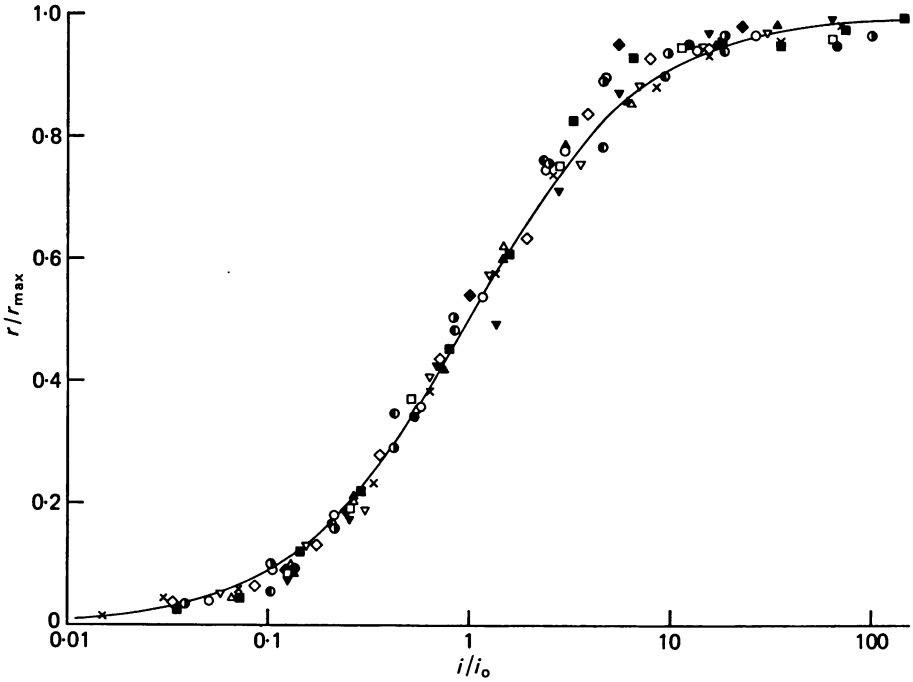

Text-fig. 4. Relation between normalized peak amplitude of the photocurrent (ordinate) and normalized flash intensity (abscissa, logarithmic scale). Collected results from thirteen cells; curve is eqn. (1). Values of r_{max} and i_0 for each cell are given in Table 1.

Eqn. (1) usually fitted the response–intensity relation, as shown in Text-fig. 4, a composite plot of the normalized relations from thirteen cells. In some cells there was a systematic deviation from eqn. (1) in that the response approached saturation more rapidly than predicted (see Text-fig. 5 for example). Table 1 gives collected values of r_{max} and i_0. The greatest value for r_{max} was 27 pA and the mean value of i_0 was 1·46 photons μm^{-2}. The wide range in r_{max} values was due in part to variations in the length of outer segment drawn into the electrode (see p. 599).

Responses to dim lights were marked by striking fluctuations (Yau *et al.* 1977) in contrast to the reproducible responses obtained previously with intracellular voltage recordings (see Fain, 1975). These variations necessitated averaging a number of small responses and contributed to uncertainty in points on the response–intensity curve. The fluctuations are treated in the subsequent paper (Baylor *et al.* 1979) and are attributed to the quantal nature of light.

Spatial contributions to response

Local and diffuse illumination

Response families to local illumination of an outer segment and diffuse illumination of the preparation are shown in Text-fig. 5*A* and *B*. The close similarity of the families is also evident in the response–intensity relations of Text-fig. 5*C*. These results are in contrast to intracellular voltage responses, which are significantly larger for diffuse light, and support the idea that the current signal represents activity predominantly of one cell.

TABLE 1. Parameters of response–intensity relations and flash response kinetics. Symbols are as in Text-figs. 4 and 9. Values of r_{max} and i_0 are those required to give the best fit of eqn. (1) to the response–intensity relations. For cells 5–13 the flash response kinetics were analysed by the method illustrated in Text-fig. 11. P, I, S indicate that the form of the best fit was: Poisson (eqn. 3), independent activation (eqn. 4), or slower decay than independent activation (see Text). All cells required $n = 4$ stages; values of t_{peak} and flash sensitivity S_f were determined from the best fit of templates. For cells 1–4, t_{peak} was determined by inspection of the average response. The ratio $i_0 S_f / r_{max}$ is expected to equal unity; it was found to range from 0·62 to 1·59. Stimuli were 20 msec flashes of 500 nm polarized light

	Response–intensity		Kinetics			
Cell	r_{max} (pA)	i_0 (photons μm^{-2})	t_{peak} (sec)	Form	Stages	S_f (pA photon^{-1} μm^2)
1 △	27	1·3	(1·1)	—	—	—
2 ▲	12	2·6	(1·1)	—	—	—
3 ▽	17	0·55	(1·4)	—	—	—
4 ▼	15·5	0·57	(2·5)	—	—	—
5 ○	20	3·3	0·6	S	4	5·6
6 ●	9·7	1·6	0·8	I	4	4·5
7 □	20	1·75	0·85	S	4	8·4
8 ■	15·3	3·0	0·9	P	4	4·9
9 ◇	22	1·0	1·2	P	4	17
10 ◆	18	0·85	1·2	S	4	15·5
11 ◐	22	0·83	1·4	I, P	4	23
12 ◑	14·5	1·1	1·55	I	4	13
13 ×	12	0·54	2·2	P	4	35·8

Mean 1·46

The expected difference in photocurrent responses between local illumination of only the recorded cell and diffuse illumination of the entire coupled network can be determined by analysing a simple electrical model. The central photoreceptor is assumed to have the equivalent circuit proposed by Baylor & Fuortes (1970), with its interior tightly coupled by low resistance junctions to a large number of identical cells. For a diffuse stimulus, the existence of coupling can be ignored as no current flows between cells, while for a local stimulus the coupling clamps the interior of the central cell at the dark potential. If the relation between light intensity and fraction of channels blocked is the Michaelis relation given by Baylor *et al.* (1974), eqn. (15), then the relation between light intensity and recorded current is also

Michaelis in the two cases. It may then be shown that the half-saturating intensities i_{diffuse} and i_{local} are related by

$$\frac{i_{\text{diffuse}}}{i_{\text{local}}} = a = 1+\frac{g_D}{G}, \tag{2}$$

where g_D is the dark value of the light-sensitive conductance and G is the conductance of the remainder of the cell. In turtle cones, the factor a has a value of about 1·6 (Baylor *et al.* 1974).

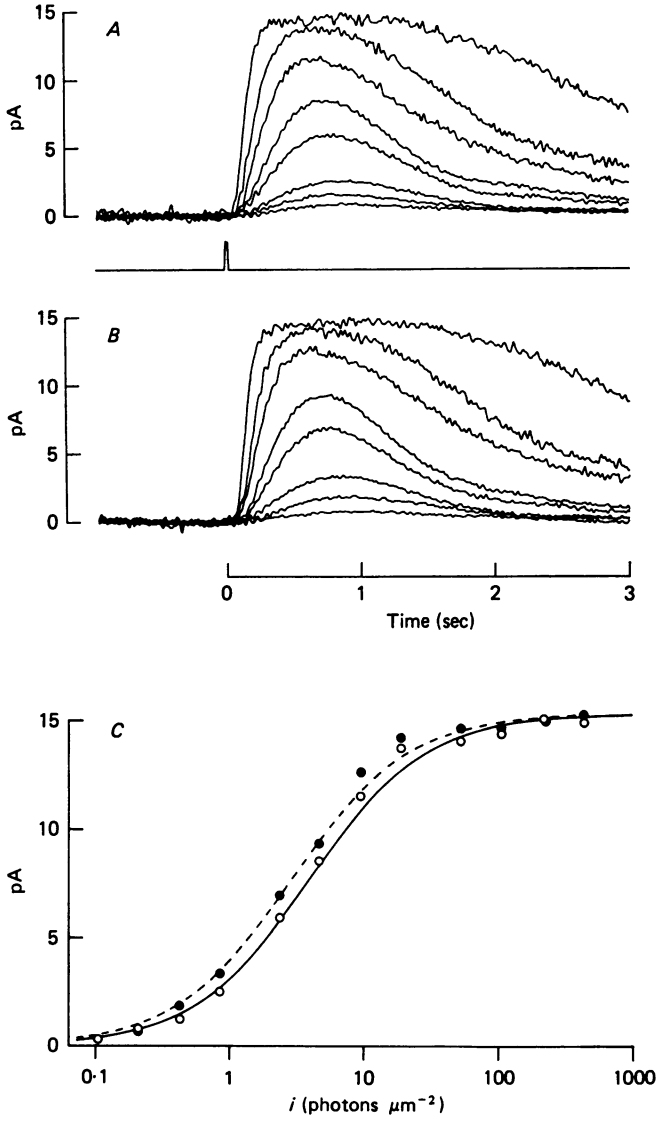

Text-fig. 5. Comparison of responses to local and diffuse flashes. Superimposed responses to 20 msec flashes of polarized 500 nm light delivering from 0·21 to 53 photons μm^{-2}. Cell 8 of Table 1. *A*, local illumination with longitudinal slit 57 μm wide and 130 μm long. *B*, diffuse illumination. *C*, response–intensity relations for local (○) and diffuse (●) light; curves are eqn. (1) with r_{max} = 15·3 pA and with i_0 = 4·0 photons μm^{-2} (continuous) and i_0 = 3·0 photons μm^{-2} (dashed).

Eqn. (2) indicates that, when photocurrent is recorded from a cell, the expected response–intensity curve with diffuse light is shifted to *higher* intensities (by about 0·2 log units if $a = 1{\cdot}6$ for rods). This predicted behaviour, which is opposite to that of intracellular voltage responses, results from the fact that in diffuse light the network hyperpolarizes, causing an inward component of current. In Text-fig. 5*C*, however, the diffuse light relation is shifted to lower intensities by about 0·1 log units. A discrepancy of this kind was observed in several experiments and probably indicates that light scattering reduced the effective intensity of the local stimulus.

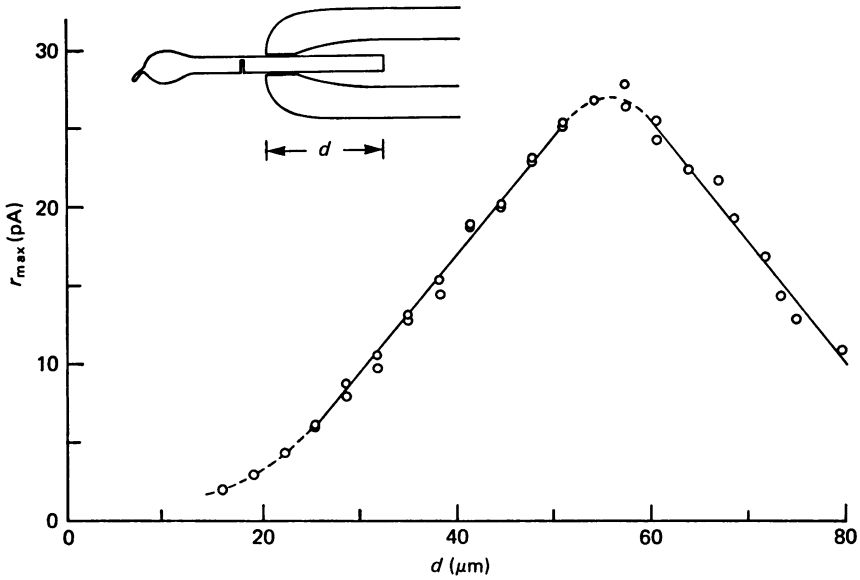

Text-fig. 6. Saturating light response as a function of length of outer segment drawn into the pipette. Ordinate is response to a diffuse 20 msec 500 nm flash delivering 64 photons μm^{-2}. Abscissa, *d*, is distance from electrode tip to distal tip of outer segment (see inset). The cell was expelled and drawn in twice, and most points are averages of two measurements. During the experiment the response at the optimal position ($d = 58\ \mu m$) decayed from 26·8 to 22·4 pA and all points have been scaled to give 26·8 pA at this position. Curve fitted by eye. This cell was completely separated from the retina (see text).

Current density along length of outer segment

To investigate the uniformity of the membrane current density in different regions of the outer segment, varying lengths of a cell were drawn into the pipette and bright diffuse light stimuli were applied. Text-fig. 6 shows results from such an experiment. Because of the finite extent of the constricted region of the pipette it was difficult to define the exact length of cell 'effectively' inside the electrode, and the distance, *d*, was measured from the distal tip of the outer segment to the tip of the pipette (see inset in Text-fig. 6). The position $d = 18\ \mu m$ on the abscissa corresponds to the tip of the outer segment being near the centre of the constriction. The saturating response increased linearly in the range $d = 24$–$52\ \mu m$, as would be expected if the current density had an approximately constant value of about 0·75 pA μm^{-1} in each element of outer segment. The deviation from linearity at small

values of d probably resulted from a lowered electrode resistance when the constriction was not fully occupied. When part of the inner segment was also drawn in, the response began to decline and the position of the maximum (d = 57 μm) occurred when the ciliary neck separating the inner and outer segments was centred in the constricted region of the pipette.

The cell illustrated in Text-fig. 6 was unusual in that the inner segment had separated completely from the more proximal synaptic ending and from other cells. This made the cell convenient for the experiment as it could readily be moved back and forth in the pipette without distortion resulting from failure of the bulk of the retina to move. In addition, it was possible to draw in the inner segment without damage, and the run only ended when the entire cell rushed into the electrode. Results from three other cells showed similar linear behaviour, but did not permit observation of the contribution of the inner segment. The mean current density for the four rods was $0{\cdot}54 \pm 0{\cdot}09$ (S.E. of mean) pA μm^{-1}.

The linearity of response amplitude with length recorded, and the implication that each element of outer segment contributed approximately equally to the saturating response confirms results of Hagins *et al.* (1970). They showed that the extracellular voltage gradient in retinal slices increased approximately linearly with distance from the distal tips of the outer segments, implying that the current density across the outer segment membrane was uniform.

Spectral sensitivity

Text-fig. 7 shows the normalized spectral sensitivity of four rods in the range 420–700 nm. The relation is similar to results obtained by Harosi (1975) with microspectrophotometry, and by Fain *et al.* (1976), and Cervetto, Pasino & Torre (1977) with intracellular recording. At 700 nm the sensitivity was reduced by nearly five orders of magnitude. The accuracy of points at such low sensitivities depends on the stop-band properties of the interference filters; tests showed that the 700 nm filter attenuated wavelengths between 500 and 580 nm by more than a factor of 10^6, indicating that sensitivities down to 10^{-5} should be reliable (see Methods, p. 590). The solid curve is the 'new' Dartnall nomogram for a retinal$_1$-based pigment with λ_{max} = 498 nm (Wyszecki & Stiles, 1967, p. 584) and provides a good fit. In the same preparation Harosi (1975) obtained a value of λ_{max} = 502 nm using microspectrophotometry, but this value gave a poorer fit to our data, and we are unable to account for the difference.

The suction technique combines some of the advantages of both electrical and microspectrophotometric measurements of spectral sensitivity. Electrical recording allows the spectrum to be followed much further down the curve than is possible with spectrophotometry, where the signal is usually lost in noise for wavelengths at which the absorbance is reduced more than about 50-fold from the peak value. In addition, in comparison with recordings in the intact retina, self-screening and filtering by other cells or structures such as oil-droplets are avoided, as the light can be confined to a single cell and the path through the outer segment is short, at right angles to the long axis. As a result, the suction electrode technique may permit the nomogram to be extended to longer wavelengths; the broken part of the curve in Text-fig. 7 illustrates the form it may take for λ_{max} = 498 nm.

Time course of the response

Absence of early transient in bright flash response

Intracellular voltage responses of cones and rods to bright flashes commonly show a rapid hyperpolarization followed almost immediately by relaxation to a plateau level (Baylor *et al.* 1971; Kleinschmidt, 1973; Schwartz, 1973; Brown & Pinto, 1974; Baylor *et al.* 1974; Fain, 1975), and a number of investigators (see

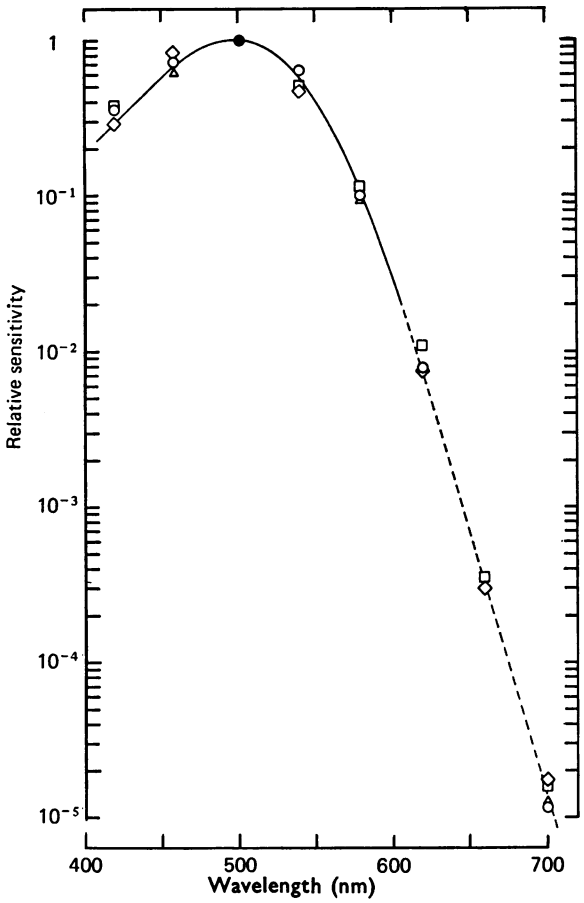

Text-fig. 7. Collected spectral sensitivities from four 'red' rods. Relative quantum sensitivity, determined in the manner described by Baylor & Hodgkin (1973), plotted logarithmically against wavelength. Each set of points was normalized to a value of unity at 500 nm. Continuous portion of curve is a Dartnall nomogram with λ_{max} = 498 nm; dashed continuation fitted by eye.

Fain, Quandt, Bastian & Gerschenfeld, 1978) give evidence that the relaxation arises from a voltage-sensitive conductance increase. A prominent decline from an initial peak was never observed in our recordings of membrane current (see, for example, Text-fig. 2*A*), although on some occasions the brightest flashes gave a small transient decrease after the initial rise. The absence of the phenomenon suggests that the ionic channels responsible for producing this phase of the voltage

change are not located in the outer segment but are instead situated more proximally, in the inner segment or synaptic ending. Although intracellular voltage might be expected to affect outer segment current, this would not be the case in bright light, when all outer segment channels are closed and the current is reduced to zero (see p. 609).

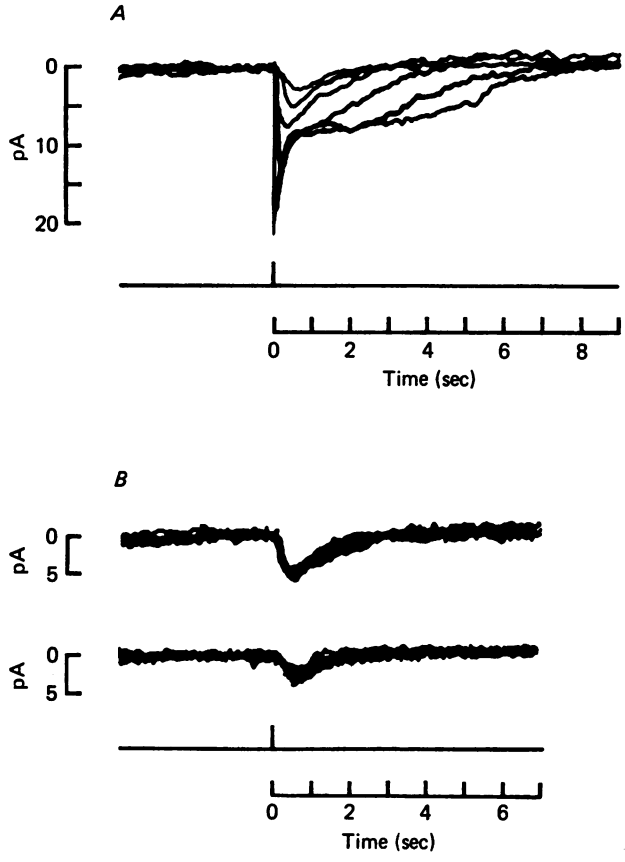

Text-fig. 8. 'Pseudo-intracellular' responses of a rod to diffuse 20 msec flashes of polarized 500 nm light. The outer segment was presumably damaged (see text). *A*, superimposed responses to flashes delivering from 0·22 to 113 photons μm^{-2}. *B*, superimposed responses to eleven (above) and fourteen (below) consecutive flashes delivering 0·45 and 0·22 photons μm^{-2} respectively.

It might be argued that the mechanism producing the transient was for some reason absent from cells in our preparation, but occasionally we recorded responses which appeared closely related to intracellular responses and which exhibited the transient. An example is shown in Text-fig. 8. When first drawn in, the cell's response to diffuse light was biphasic, with a rapid inward transient followed by a slower outward component, but after a short time the second component disappeared, leaving purely negative-going responses as illustrated in the family of Text-fig. 8*A*. These responses to diffuse light are very similar to intracellular voltage records, suggesting that they represent a measure of intracellular voltage. A possible explanation is that the cell membrane was punctured at a position distal to the

electrode constriction, abolishing the light-evoked conductance change in the recorded outer segment but allowing a current change due to hyperpolarization of other rods coupled to the central cell. On one occasion a normal outward photocurrent without a transient was observed from a cell, while an adjacent outer segment recorded immediately afterwards showed the inverted response with a prominent transient. Similar inverted responses with an early peak were recorded from three other rods.

Text-fig. 8*B* shows that responses to dim diffuse flashes recorded 'intracellularly' in our preparation showed little variation in amplitude, in contrast to the fluctuations observed in the current recordings (Yau *et al.* 1977; Baylor *et al.* 1979). Such constancy would be expected of responses representing the average voltage in a network of coupled cells (see Fain, 1975; Lamb & Simon, 1976; Schwartz, 1976).

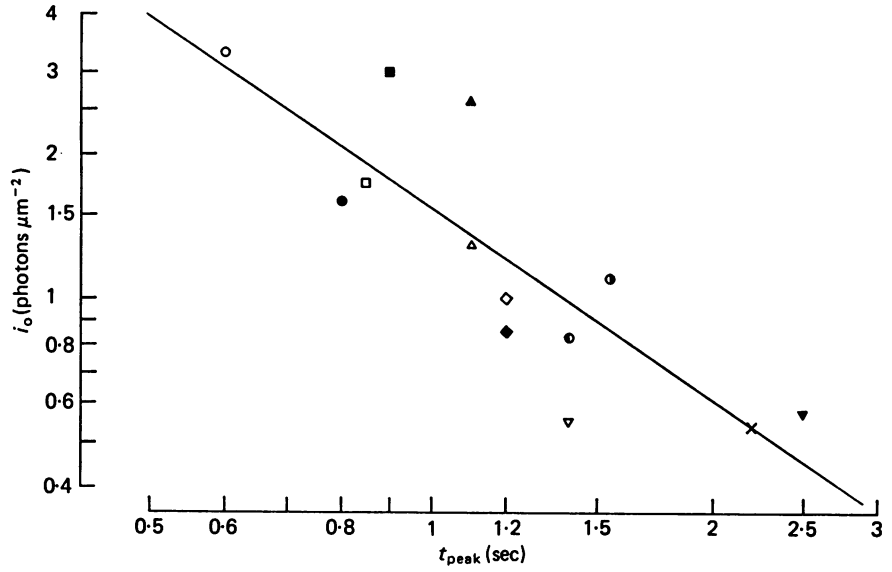

Text-fig. 9. Relation between half-saturating intensity, i_0, and time to peak of the dim flash response, t_{peak}; logarithmic scales. Same cells as Text-fig. 4 and Table 1. Straight line is $i_0 \propto t_{peak}^{-1.34}$, representing the linear regression of log i_0 to log t_{peak}; correlation coefficient 0·84.

Time to peak

In different cells the time to the peak of the dim flash response, t_{peak}, varied between 0·6 and 4 sec. In many cases the slower cells were more sensitive although the saturating amplitudes were similar. This relation is illustrated by Text-fig. 9, in which the half-saturating intensity i_0 is plotted against t_{peak} in logarithmic coordinates for the cells of Table 1. The straight line is the regression fit of log i_0 to log t_{peak} and describes a power law relation $i_0 \propto t_{peak}^{-1.34}$. Previous intracellular studies in the same preparation gave the time to the peak of the dim flash response as about 1 sec (Brown & Pinto, 1974; Fain, 1975) or about 0·4 sec (Cervetto *et al.* 1977), similar to that of the faster responses obtained here. It seems odd that the slower responses, which might at first be thought to be unphysiological, corresponded to considerably higher sensitivities. Changes in an 'integrating' step might explain

the correlation; for example, slowing the rate of removal of internal transmitter could slow the kinetics and increase the sensitivity.

It is possible that the slowness resulted in part from inadequate oxygenation or from deterioration of the cells; during the course of an experiment the time to peak sometimes increased. In early experiments the Ringer solution was thoroughly oxygenated only initially, and not during recording. Later the method shown in Text-fig. 1*B* was adopted, in which a stream of moist oxygen was directed across the Ringer surface, to oxygenate and gently stir the solution. In these later experiments very slow cells were encountered less frequently. It is also possible that the procedure of cutting the retina into small pieces may have slowed the responses. Results in this paper are taken only from cells in which t_{peak} was less than 2·5 sec.

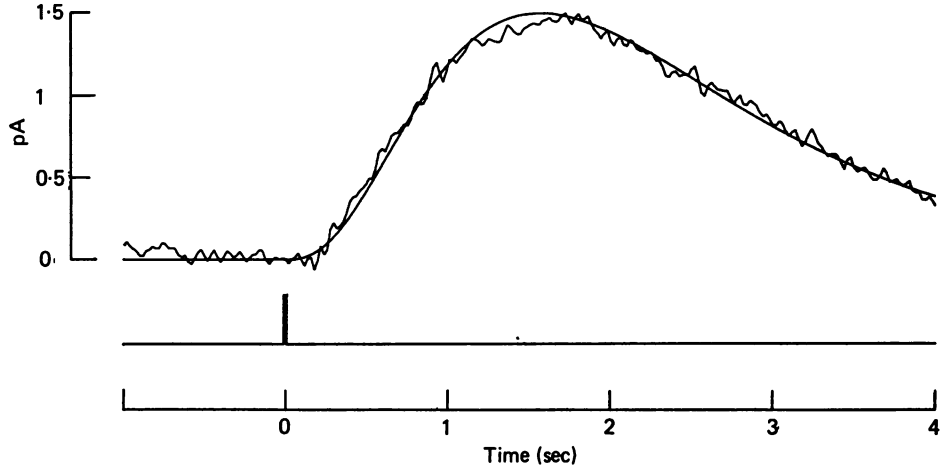

Text-fig. 10. Average response to dim flashes. Linear plot of average response (noisy trace) to local flashes delivering 0·11 photons μm^{-2}; forty trials. Smooth curve is redrawn from Text-fig. 11; eqn. (4), $n = 4$, $t_{peak} = 1{\cdot}55$ sec, $r = 1{\cdot}5$ pA. Cell 12 of Table 1.

Kinetics of the response

The average response of a cell to dim flashes is shown in Text-fig. 10 (noisy trace). Its shape appears similar to that seen previously in intracellular voltage recordings from photoreceptors. To fit the response we used the procedure of Baylor *et al.* (1974) in which the response divided by stimulus intensity is plotted as a function of time in double logarithmic co-ordinates. This method has the dual advantage that stereotyped templates can be used to test the fit and that the applicability of theoretical equations can be tested at early times in the response. Responses of the cell at twelve intensities are plotted in Text-fig. 11 using this procedure.

The curves used in attempts to fit the response were two of those used by Baylor *et al.* (1974), the *Poisson* and *independent activation* cases. Their eqns. (44) and (38) are rewritten here in normalized form as

(Poisson) $$r^*(t) = iS_f T^{n-1} e^{(n-1)(1-T)} \tag{3}$$

and

(Independence) $$r^*(t) = iS_f \frac{n^n}{(n-1)^{n-1}} n^{-T}(1-n^{-T})^{n-1}. \tag{4}$$

Here $r^*(t)$ is the linear response (i.e. before allowing for compression by saturation), i is flash intensity (photons μm^{-2}), S_f is flash sensitivity (pA photon^{-1} μm^2), n is the number of delay stages and T is normalized time ($T = t/t_{peak}$). (Note that for $T = 1$ the terms involving n and T in eqns. (3) and (4) reduce to unity.)

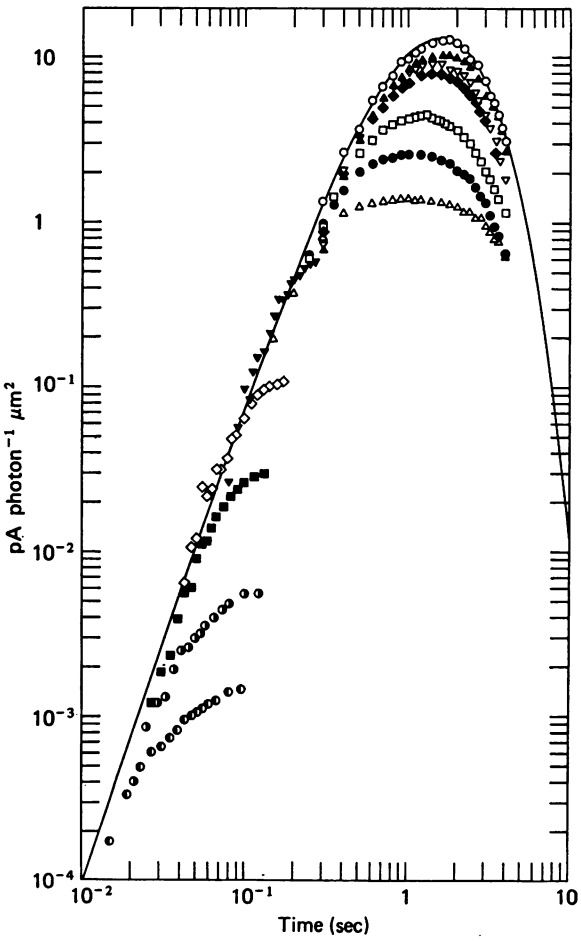

Text-fig. 11. Kinetics of outer segment photocurrent. Double logarithmic plot of response divided by intensity for cell illustrated in Text-fig. 10. Each symbol represents a different intensity, from 0·11 photons μm^{-2} (○, same responses as in Text-fig. 10) to $1{\cdot}1 \times 10^4$ photons μm^{-2} (◐). Curve is eqn. (4) with $n = 4$, $t_{peak} = 1{\cdot}55$ sec, $S_f = 13$ pA photon^{-1} μm^2. Cell 12 of Table 1. Responses to the five highest intensities (▼, ◇, ■, ◑, ◐) were not filtered; other responses were filtered by a 20 Hz 6-pole low-pass filter.

The points at early times (i.e. in the linear range) of each response in Text-fig. 11 could be fitted by eqn. (4) with $n = 4$ and $t_{peak} = 1{\cdot}55$ sec, but eqn. (3) did not provide a very good fit. The curve has been redrawn in the linear co-ordinates of Text-fig. 10 and provides a good fit. The time constants of the four delay stages involved in this particular fit are 1120, 560, 370, and 280 msec.

For the very bright lights (i.e. symbols towards the bottom) the curve lies to the left of the symbols. Correction for the finite flash width would shift the curve in

this region further to the left, while correction for the electrical time constant of the cell would shift the curve to the right. Preliminary analysis of responses to the brightest lights suggested that the rise was limited by a time constant of about 30–40 msec. This means that in addition to the four time constants, there was another of 30–40 msec which was only apparent with very bright lights. This may represent the electrical time constant of the cell, although it is substantially longer than the 9 msec estimated by Schwartz (1976) for rods in the turtle.

Parameters estimated from the flash response kinetics are collected in Table 1 for nine cells. In all cases the fit was best with $n = 4$ stages, as found by Penn & Hagins (1972) in rat rods, but in contrast to the case of $n = 6$ in turtle cones (Baylor *et al.* 1974) and turtle rods (Schwartz, 1976). Different cells were best fitted either by eqn. (3) (P – Poisson), by eqn. (4) (I – independent activation) or by a similar rising phase but slower falling phase than independence (S). We did not attempt to fit this last class exactly, but it seems likely that a curve of the type of eqn. (43) of Baylor *et al.* (1974) may be applicable. We conclude that the response kinetics are well described by four time constants in the range 200–1200 msec.

Time course of response to stimulation at different positions on outer segment

Text-fig. 12*A* shows averaged responses to dim flashes of two intensities presented locally at different positions on an outer segment. A transverse slit stimulus 9·6 μm wide was flashed near the tip of the outer segment (traces 1 and 2) and at a position 32 μm nearer its base (traces 3 and 4). The responses elicited from the base reached peak about 1 sec earlier than those from the tip, and it is apparent that the faster responses were not the result of differences in amplitude at the two positions. The different kinetics at tip and base were found in all cells examined, as shown in Text-fig. 12*B*. Here t_{peak} obtained with a flash of fixed intensity is plotted against stimulus position on the outer segment. It is clear that in spite of variations in the time scale of different cells the response at the basal end of the outer segment was consistently faster than that at the distal tip.

In Text-fig. 12*A* flashes of the same intensity (traces 1 and 3) gave larger responses when presented at the tip. This was not a consistent finding and in other experiments a given intensity gave a larger response at the basal end than at the tip. It is not clear whether the differences in apparent sensitivity were caused by differences in effective intensity (perhaps resulting from the variable thickness of glass in the pipette), by imperfect collection of current near the constriction, or by real differences in sensitivity along the outer segment.

Effect of background light on time course of response

Baylor & Hodgkin (1974) showed that background illumination accelerated the intracellular voltage response of cones to dim incremental flashes. Text-fig. 13 shows the same effect in the current responses of a rod outer segment. The trace labelled 1 is the average response to a dim flash presented in darkness, while traces 2 and 3 are responses to flashes presented during background illumination. (In order to maintain a nearly constant response amplitude the flash intensity was increased for traces 2 and 3.) The response acceleration was considerable, as t_{peak} dropped from 1·5 sec to 0·5 sec with a background which gave an average response of 6·8 pA

(about 45% maximal). The observation that the acceleration affects membrane current as well as intracellular voltage supports the notion (Baylor & Hodgkin, 1974) that the altered wave form represents a change in the state of the transduction mechanism within the outer segment.

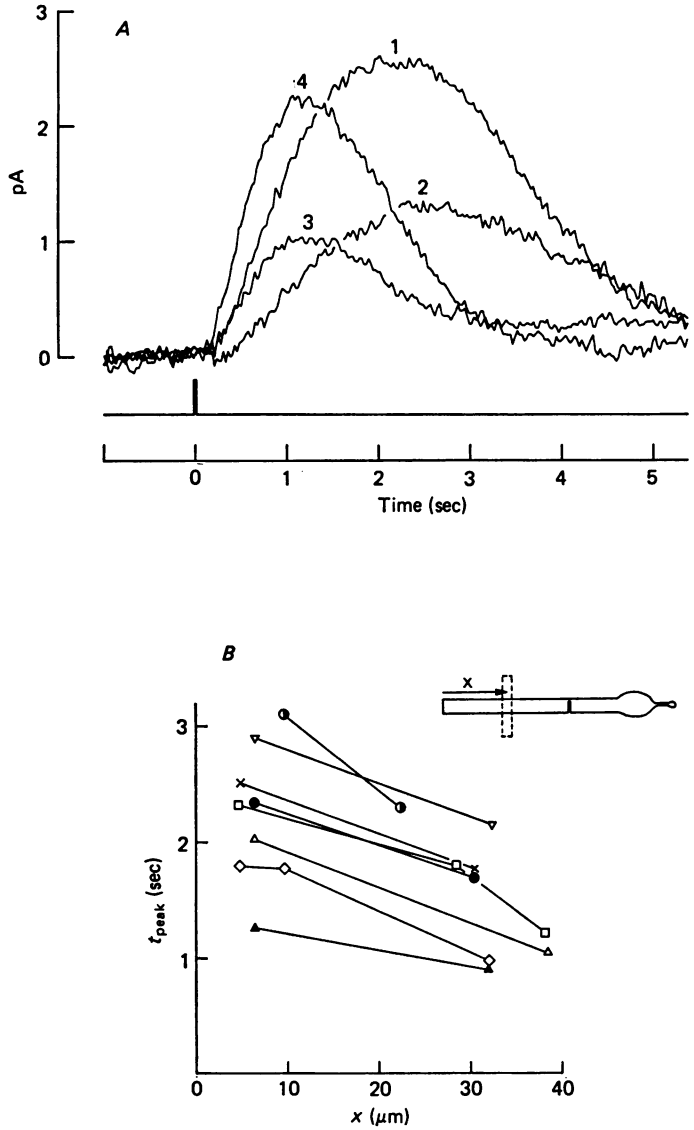

Text-fig. 12. Time course of the response at the tip and base of the outer segment. *A*, averaged flash responses to a narrow transverse slit near the tip (traces 1, 2) or nearer the base (traces 3, 4). Distance of stimulus from tip of outer segment, incident intensity (in photons μm^{-2}) and number of trials averaged were respectively, trace 1: 6·4 μm, 0·85, thirty; trace 2: 6·4 μm, 0·43, thirty-one; trace 3: 38·3 μm, 0·85, thirty-nine; trace 4: 38·3 μm, 2·4, twenty-six. Slit width 9·6 μm, 500 nm, 20 msec flash; total length of outer segment 70 μm. Cell 9 of Table 1. *B*, time to peak of dim flash response, t_{peak}, plotted against distance, x, of stimulus from tip of outer segment (see inset); collected results from eight cells. For a given cell the values of t_{peak} were determined at the same intensity; all response amplitudes less than 2·5 pA.

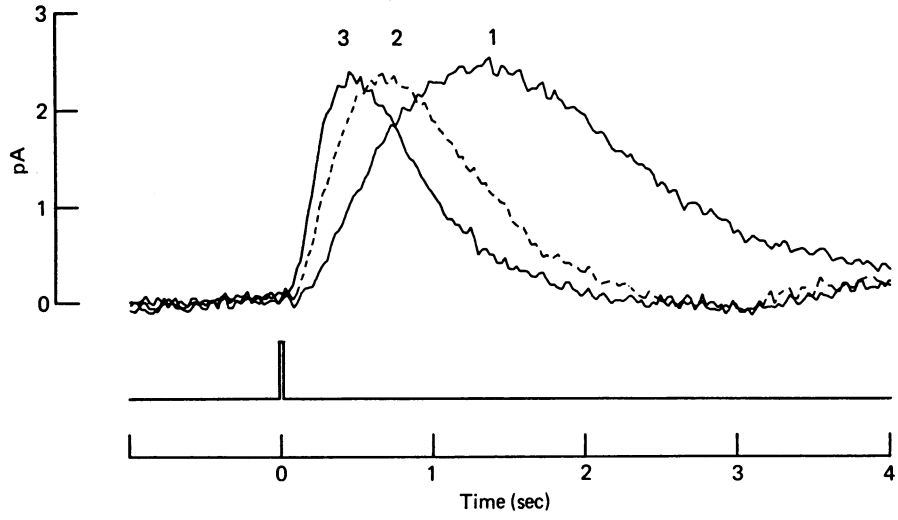

Text-fig. 13. Acceleration of flash response by background illumination. Superimposed averaged responses of a cell to 20 msec flashes of 520 nm light in the presence of a 500 nm steady background. Background intensity in photons μm^{-2} sec^{-1}, average steady response, flash intensity in photons μm^{-2} and number of trials averaged were respectively, curve 1: no background, 0 pA, 0·12, thirty-five; curve 2: 0·51, 5·2 pA, 0·59, thirty-three; curve 3: 2·1, 6·8 pA, combined 1·2, twenty and 2·5, six. Saturating response 15 pA.

DISCUSSION

In certain respects light responses obtained by recording outer segment membrane current and intracellular voltage are comparable. Both show: (i) a response–intensity relation described by eqn. (1) with half-saturating intensity about 1 photon μm^{-2}, (ii) an S-shaped delay involving a series of steps, (iii) acceleration of the response by adapting lights and (iv) a spectral sensitivity described by a Dartnall (1968) nomogram with λ_{max} near 500 nm. The similarities are expected for effects resulting directly from the transduction process in the outer segment.

A significant difference involves the absence in the current recordings of a transient component in the response to bright flashes, despite demonstration that the mechanism responsible for the intracellular voltage transient was still present. We interpret this difference to indicate that the conductance change generating the transient is not located in the outer segment but instead in a more proximal region of the cell (however, see Cervetto *et al.* 1977).

A second difference involves the effects of local and diffuse illumination. In voltage recordings the response–intensity relation depends strongly on the area of the light stimulus, and Fain (1975) has estimated that about 90% of the response of a toad rod to diffuse light is generated in cells electrically coupled to it. With current recordings the effects of local and diffuse illumination were almost indistinguishable. The explanation for the different results with the two methods is that the current responses reflect primarily events occurring in the recorded outer segment. This property has the consequence that fluctuations are more pronounced in recordings

of current across a single outer segment than in voltage recordings; use is made of this in a following paper (Baylor *et al.* 1979) to study the effects of single photons.

It is interesting to compare the maximum current density flowing across the outer segment membrane with that flowing in nerve during an action potential. The outer segment dark current is roughly 25 pA and its surface area is roughly 1200 μm^2 ($\pi \times 6\ \mu m \times 60\ \mu m$) giving a current density of 2 $\mu A\ cm^{-2}$. In contrast, the maximum current density during the rising phase of the action potential in the squid axon is about 2 $mA\ cm^{-2}$ (Hodgkin & Huxley, 1952), three orders of magnitude larger. The great difference suggests that there may be a considerable difference in channel density or in channel properties between the two membranes.

The absence of net outer segment current during bright light does not itself indicate that the membrane conductance is zero. However, a residual conductance would permit a component of current to flow during the sag of intracellular voltage from its initial peak. Such a component, which would add to the early photocurrent, was not detectable in our experiments, and we estimate any residual conductance in the outer segment to be less than about 10% of the light-sensitive conductance.

As in previous intracellular recordings, flash responses were progressively reduced in size and shortened in duration by background lights of increasing intensity. This phenomenon indicates that the transduction mechanism within the outer segment undergoes adaptational change. Other factors, such as changes in voltage-sensitive conductance in the inner segment, which might contribute to the effect in intracellular voltage, can be ruled out as they would generate current components giving the opposite effect. In cones the alteration in transduction can be accounted for by assuming that backgrounds increase the rate constant of the step which terminates action of the internal transmitter (Baylor & Hodgkin, 1974).

The time course of the rod reponses reported here is somewhat slower than in previous intracellular studies (Brown & Pinto, 1974; Fain, 1975; Cervetto *et al.* 1977) and may indicate that our preparation was more fully dark adapted. In addition, with intracellular methods the light is incident from the vitreal side of the retina approximately axially to the outer segment, so that much of the absorption is at the basal end. As stimulation of more basal regions elicits faster responses (Text-fig. 12) one would expect the time course to be faster with axial illumination than with uniform illumination from a transverse direction. It is also possible that the conductance change generating the transient voltage response to bright lights may exert some effect even on small signals (see Schwartz, 1976; Detwiler, Hodgkin & McNaughton, 1978). This would diminish the late phase of the linear voltage response, thus causing it to be faster than the light-sensitive conductance change. To examine this it would be useful to record voltage and current simultaneously from the same cell.

The different response kinetics at tip and base could not result from longitudinal diffusion of internal transmitter from the site of absorption to the base of the outer segment, because experiments (see p. 599) showed that each element of surface membrane contributed equally to the response. Instead it seems likely that the kinetics of liberation or removal of internal transmitter vary systematically with disk location. One possibility is the existence of a gradient of a diffusable metabolite which originates in mitochondria in the inner segment and which plays a role in

controlling the concentration of internal transmitter. An alternative is the 'ageing' of a membrane constituent as the disks migrate along the outer segment from their site of generation at the base to their site of removal at the tip (Young & Droz, 1968).

We wish to thank Mr G. Kuhn for excellent technical assistance. This work was supported by grant EY-05143 from the National Eye Institute, USPHS, by grants from the Sloan and Sinsheimer Foundations, and by a Bank of America–Giannini Fellowship to K.W.Y.

REFERENCES

BAYLOR, D. A. & FUORTES, M. G. F. (1970). Electrical responses of single cones in the retina of the turtle. *J. Physiol.* **207**, 77–92.

BAYLOR, D. A., FUORTES, M. G. F. & O'BRYAN, P. M. (1971). Receptive fields of cones in the retina of the turtle. *J. Physiol.* **214**, 265–294.

BAYLOR, D. A. & HODGKIN, A. L. (1973). Detection and resolution of visual stimuli by turtle photoreceptors. *J. Physiol.* **234**, 163–198.

BAYLOR, D. A. & HODGKIN, A. L. (1974). Changes in time scale and sensitivity in turtle photoreceptors. *J. Physiol.* **242**, 729–758.

BAYLOR, D. A., HODGKIN, A. L. & LAMB, T. D. (1974). The electrical response of turtle cones to flashes and steps of light. *J. Physiol.* **242**, 685–727.

BAYLOR, D. A., LAMB, T. D. & YAU, K.-W. (1979). Responses of retinal rods to single photons. *J. Physiol.* **288**, 613–634.

BROWN, J. E. & PINTO, L. H. (1974). Ionic mechanism for the photoreceptor potential of the retina of *Bufo marinus*. *J. Physiol.* **236**, 575–591.

CERVETTO, L., PASINO, E. & TORRE, V. (1977). Electrical responses of rods in the retina of *Bufo marinus*. *J. Physiol.* **267**, 17–51.

COPENHAGEN, D. R. & OWEN, W. G. (1976). Coupling between rod photoreceptors in a vertebrate retina. *Nature, Lond.* **260**, 57–59.

DARTNALL, H. T. A. (1968). The photosensitivities of visual pigments in the presence of hydroxylamine. *Vision Res.* **8**, 339–358.

DETWILER, P. B., HODGKIN, A. L. & MCNAUGHTON, P. A. (1978). A surprising property of electrical spread in the network of rods in the turtle's retina. *Nature, Lond.* **274**, 562–565.

FAIN, G. L. (1975). Quantum sensitivity of rods in the toad retina. *Science, N.Y.* **187**, 838–841.

FAIN, G. L., GOLD, G. H. & DOWLING, J. E. (1976). Receptor coupling in the toad retina. *Cold Spring Harb. Symp. quant. Biol.* **40**, 547–561.

FAIN, G. L., QUANDT, F. N., BASTIAN, B. L. & GERSCHENFELD, H. M. (1978). Contribution of a caesium-sensitive conductance increase to the rod photoresponse. *Nature, Lond.* **272**, 467–469.

HAGINS, W. A., PENN, R. D. & YOSHIKAMI, S. (1970). Dark current and photocurrent in retinal rods. *Biophys. J.* **10**, 380–412.

HAROSI, F. I. (1975). Absorption spectra and linear dichroism of some amphibian photoreceptors. *J. gen. Physiol.* **66**, 357–382.

HODGKIN, A. L. & HUXLEY, A. F. (1952). A quantitative description of membrane current and its application to conduction and excitation in nerve. *J. Physiol.* **117**, 500–544.

JAGGER, W. S. (1976). Receptor potentials from single isolated frog rods. *Eur. J. Physiol.* **362**, (suppl.), R47.

KLEINSCHMIDT, J. (1973). Adaptation properties of intracellularly recorded Gekko photoreceptor potentials. *Biochemistry and Physiology of Visual Pigments*, pp. 219–224. Berlin: Springer.

LAMB, T. D. & SIMON, E. J. (1976). The relation between intercellular coupling and electrical noise in turtle photoreceptors. *J. Physiol.* **263**, 257–286.

LAMB, T. D. & SIMON, E. J. (1977). Analysis of electrical noise in turtle cones. *J. Physiol.* **272**, 435–468.

MCBURNEY, R. N. & NORMANN, R. A. (1977). Current and voltage responses from single rods in toad retina. *J. gen. Physiol.* **70**, 12*a*.

NEHER, E. & SAKMANN, B. (1976). Single-channel currents recorded from membrane of denervated frog muscle fibres. *Nature, Lond.* **260**, 799–802.

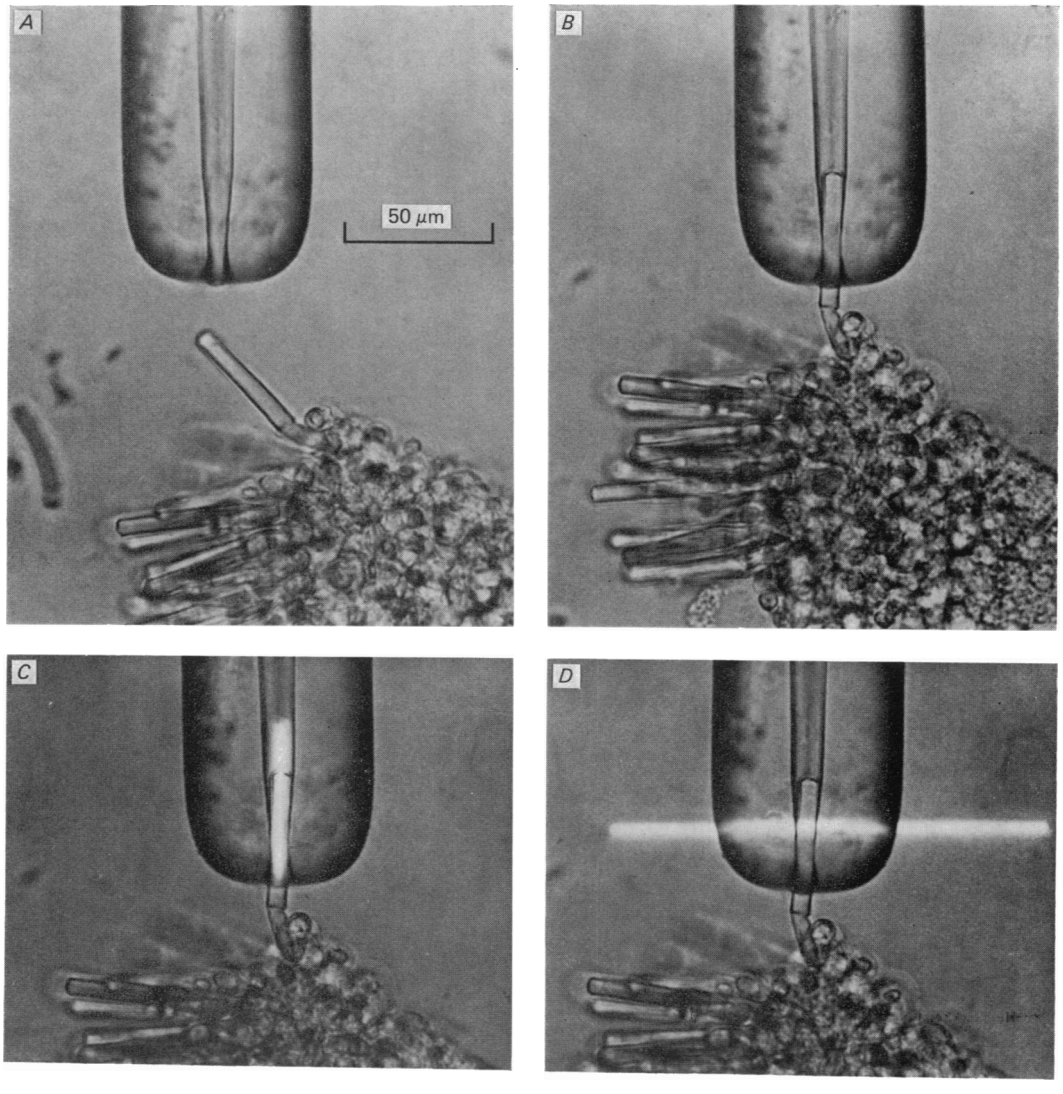
A
50 μm
B
C
D

PENN, R. D. & HAGINS, W. A. (1972). Kinetics of the photocurrent of retinal rods. *Biophys. J.* **12**, 1073–1094.

SCHWARTZ, E. A. (1973). Responses of single rods in the retina of the turtle. *J. Physiol.* **232**, 503–514.

SCHWARTZ, E. A. (1976). Electrical properties of the rod syncytium in the retina of the turtle. *J. Physiol.* **257**, 379–406.

SCHWARTZ, E. A. (1977). Voltage noise observed in rods of the turtle retina. *J. Physiol.* **272**, 217–246.

SIMON, E. J., LAMB, T. D. & HODGKIN, A. L. (1975). Spontaneous voltage fluctuations in retinal cones and bipolar cells. *Nature, Lond.* **256**, 661–662.

TOMITA, T. (1970). Electrical activity of vertebrate photoreceptors. *Q. Rev. Biophys.* **3**, 179–222.

WYSZECKI, G. & STILES, W. S. (1967). *Color Science. Concepts and Methods, Quantitative Data and Formulas.* New York: John Wiley & Sons.

YAU, K.-W., LAMB, T. D. & BAYLOR, D. A. (1977). Light-induced fluctuations in membrane current of single toad rod outer segments. *Nature, Lond.* **269**, 78–80.

YOUNG, R. W. & DROZ, B. (1968). The renewal of protein in retinal rods and cones. *J. cell Biol.* **39**, 169–184.

EXPLANATION OF PLATE

Photomicrographs showing suction electrode, 'red' rod projecting from piece of retina, and light stimuli.

A, preparation approaching tip of electrode.

B, outer segment of rod in position. Proximal end of cell remains attached to retina. Boundary between inner and outer segments is visible.

C, longitudinal slit of 500 nm light on outer segment, nominal slit width 2·5 μm.

D, same, but slit oriented transversely.

Micrographs made in 500 nm light through camera tube of inverted microscope.